Multi-particle structure in the Z_n-chiral Potts models

1993 J. Phys. A: Math. Gen. 26 1275

(http://iopscience.iop.org/0305-4470/26/6/012)

J. Phys. A: Math. Gen. 26 (1993) 1275–1298. Printed in the UK

Multi-particle structure in the $\mathbb{Z}_n$-chiral Potts models

G von Gehlen† and A Honecker‡

Physikalisches Institut der Universität Bonn, Nußallee 12, D 5300 Bonn 1, Federal Republic of Germany

Received 29 October 1992

Abstract. We calculate the lowest translationally invariant levels of the $\mathbb{Z}_3$- and $\mathbb{Z}_4$-symmetrical chiral Potts quantum chains, using numerical diagonalization of the Hamiltonian for $N \leqslant 12$ and $N \leqslant 10$ sites, respectively, and extrapolating $N \to \infty$. In the high-temperature massive phase we find that the pattern of the low-lying zero momentum levels can be explained assuming the existence of $n-1$ particles carrying $\mathbb{Z}_n$ charges $Q = 1, \ldots, n-1$ (mass m_Q), and their scattering states. In the superintegrable case the masses of the $n-1$ particles become proportional to their respective charges: $m_Q = Qm_1$. Exponential convergence in N is observed for the single-particle gaps, while power convergence is seen for the scattering levels. We also verify that qualitatively the same pattern appears for the self-dual and integrable cases. For general $\mathbb{Z}_n$ we show that the energy–momentum relations of the particles show a parity non-conservation asymmetry which for very high temperatures is exclusive due to the presence of a macroscopic momentum $P_m = (1 - 2Q/n)\phi$, where ϕ is the chiral angle and Q is the $\mathbb{Z}_n$ charge of the respective particle.

1. Introduction

The $\mathbb{Z}_3$-chiral Potts model was introduced in 1981 by Ostlund [1] and Huse [2] in order to describe incommensurate phases of physisorbed systems, e.g. monolayer krypton on a graphite surface [3]. The phase structure of several versions of the model has been studied by various methods: mean-field, Monte Carlo, renormalization group, transfer-matrix partial diagonalization and finite-size scaling of quantum chains [4–7]. In the following we shall focus principally on the quantum chain version of the model.

In 1981–82 quantum chain Hamiltonians for the chiral Potts model were obtained [8,9] via the τ-continuum limit [10,11] from the Ostlund–Huse two-dimensional model. These were not self-dual, so that the location of the critical manifold was possible only by finite-size scaling [6,12]. In 1983 Howes *et al* [13] introduced a self-dual $\mathbb{Z}_3$-symmetrical chiral quantum chain, which, however, does not correspond to a two-dimensional model with positive Boltzmann weights. Therefore in the self-dual model the immediate connection to realistic physisorbed systems is lost, but its peculiar mathematical structure has attracted much interest: Howes *et al* found that the lowest gap of the self-dual model is linear in the inverse temperature, and subsequently in [14] it was shown that the model fulfils the Dolan–Grady integrability

† E-mail address: unp02f@ibm.rhrz.uni-bonn.de
‡ E-mail address: unp06b@ibm.rhrz.uni-bonn.de

0305-4470/93/061275+24$07.50

conditions [15] (now usually called 'superintegrability' [16]). A whole series of $\mathbb{Z}_n$-symmetrical quantum chains has been defined, which satisfy the superintegrability conditions [14]. The Dolan–Grady integrability conditions have been shown to be equivalent to the Onsager algebra [17–19], which entails that all eigenvalues of the Hamiltonian have a simple Ising-type form. The well known Ising quantum chain in a transverse field is the $\mathbb{Z}_2$-version of the superintegrable chiral Potts models.

Much work has been done in the past few years in order to obtain analytic expressions for the complete spectrum of the $\mathbb{Z}_3$-superintegrable model [16, 20]. In the next section we shall quote some of these results. The aim of the present paper is not to add to the analytic calculations of the special superintegrable case, but rather to use numerical finite-size analysis in order to investigate, how the integrable model is embedded in the more general versions of the chiral $\mathbb{Z}_3$ and $\mathbb{Z}_4$ models. We shall study the low-lying levels of the excitation spectrum and investigate the possibility of a particle interpretation.

In the neighbourhood of conformal points of isotropic theories, very simple particle patterns have been found by Zamolodchikov's perturbation expansion [21], which is applicable to the non-chiral limit of the chiral Potts models. We shall follow these particle patterns by varying the chiral angles, and try to find out which special properties of the spectrum lead, for particular parameter values, to superintegrability. Since for this purpose we have to study the spectrum through a large probably non-integrable parameter range, at present there is no alternative to numerical methods. It turns out that even in those cases which can be solved analytically, some basic features can be discovered rather easily through a numerical calculation, because the exact formulae are quite involved.

The plan of this paper is as follows. In section 2 we start with the basic definitions of the chiral Potts model for general $\mathbb{Z}_n$ symmetry, which are then specialized to the $\mathbb{Z}_3$ and $\mathbb{Z}_4$ cases. Section 3 collects some basic analytic results which are available for the generic $\mathbb{Z}_n$-symmetric model. In section 4 we give our detailed finite-size numerical results which confirm the two-particle interpretation of the low-lying spectrum of the self-dual version of the $\mathbb{Z}_3$-model. Section 5 discusses the analogous results for the self-dual version of the $\mathbb{Z}_4$-model and shows that the low-lying spectrum is well described in terms of three elementary particles. While up to this point, we consider translationally invariant states only, in section 6 we present observations on the energy–momentum dispersion relations of the elementary particles and the effects of parity violation on the spectrum. Finally, section 7 collects our conclusions.

2. The chiral $\mathbb{Z}_n$-Potts quantum chain

The chiral $\mathbb{Z}_n$-symmetric Potts spin quantum chain [14] with N sites is defined by the Hamiltonian

$$H^{(n)} = -\sum_{j=1}^{N}\sum_{k=1}^{n-1}\{\bar{\alpha}_k\sigma_j^k + \lambda\alpha_k\Gamma_j^k\Gamma_{j+1}^{n-k}\}. \tag{1}$$

Here σ_j and Γ_j are $n \times n$ matrices acting at site j, which satisfy the relations

$$\sigma_j\Gamma_{j'} = \Gamma_{j'}\sigma_j\omega^{\delta_{j,j'}} \qquad \sigma_j^n = \Gamma_j^n = \mathbf{1} \qquad \omega = \exp(2\pi\mathrm{i}/n). \tag{2}$$

A convenient representation for σ and Γ in terms of diagonal and lowering matrices, respectively, is given by

$$(\sigma)_{l,m} = \delta_{l,m}\omega^{l-1} \qquad (\Gamma)_{l,m} = \delta_{l+1,m} \qquad (\mathrm{mod}\ n). \tag{3}$$

We shall assume periodic boundary conditions: $\Gamma_{N+1} = \Gamma_1$.

The model contains $2n-1$ parameters: the real inverse temperature λ and the complex constants α_k and $\bar{\alpha}_k$. We shall only consider the case of $H^{(n)}$ being Hermitian: $\alpha_k = \alpha^*_{n-k}$ and $\bar{\alpha}_k = \bar{\alpha}^*_{n-k}$. For $n > 2$ and generic complex α_k and $\bar{\alpha}_k$, the Perron–Frobenius theorem does not apply and the spectrum of $H^{(n)}$ may show ground-state level crossings. $H^{(n)}$ commutes with the $\mathbb{Z}_n$ charge operator $\bar{Q} = \prod_{j=1}^{N} \sigma_j$. The eigenvalues of $\bar{Q}$ have the form $\exp(2\pi \mathrm{i} Q/n)$ with Q integer. We shall refer to the n charge sectors of the spectrum of $H^{(n)}$ by $Q = 0, \ldots, n-1$, respectively. Parity is not a good quantum number, but $H^{(n)}$ is translational invariant, so that each eigenstate of $H^{(n)}$ can be labelled by its momentum eigenvalue p.

For $\alpha_k = \bar{\alpha}_k$ the model is self-dual with respect to the reflection $\lambda \to \lambda^{-1}$. If we choose [14]

$$\alpha_k = \bar{\alpha}_k = 1 - \mathrm{i}\cot(\pi k/n) \tag{4}$$

then the model is 'superintegrable' [22], i.e. it fulfils the Dolan–Grady [15] conditions and therefore the λ-dependence of all eigenvalues $E(\lambda)$ of $H^{(n)}$ has the special Ising-like form [18, 22]:

$$E(\lambda) = a + b\lambda + \sum_j 4m_j \sqrt{1 + 2\lambda\cos\theta_j + \lambda^2}. \tag{5}$$

Here a, b and θ_j are real numbers. The m_j take the values $m_j = -s_j, -s_j + 1, \ldots, s_j$, where s_j is a finite integer. For details concerning formula (5), see [18, 22].

Albertini *et al* [22, 23] have obtained a spin chain of the form (1) with

$$\alpha_k = \mathrm{e}^{\mathrm{i}(2k/n-1)\phi}/\sin(\pi k/n) \qquad \bar{\alpha}_k = \mathrm{e}^{\mathrm{i}(2k/n-1)\varphi}/\sin(\pi k/n) \tag{6}$$

$$\cos\varphi = \lambda\cos\phi \tag{7}$$

as a limiting case of an integrable two-dimensional lattice model. The Boltzmann weights of their two-dimensional model do not have the usual difference property [23] and satisfy a new type of Yang–Baxter equation which involve spectral parameters defined on Riemann surfaces of higher genus. So a quantum chain (1) with coefficients (6), (7) is integrable. The superintegrable case is contained in (6) for $\varphi = \phi = \pi/2$.

A number of analytic results is available for the superintegrable case. Some of these will be reviewed in the next section. Starting in 1987, the Stony-Brook group has published a series of papers [16, 22, 23] which give analytic calculations of the spectrum of the $\mathbb{Z}_3$-superintegrable quantum chain. Recently, the completeness of the analytic expressions for the levels of the superintegrable $\mathbb{Z}_3$-model has been shown by Dasmahapatra *et al* [24].

In the non-chiral limiting case $\varphi = \phi = 0$ of the Hamiltonian (1) with coefficients (6) we obtain the lattice version of the parafermionic $\mathbb{Z}_n$-symmetrical

Fateev–Zamolodchikov models $\mathcal{WA}_{n-1}$ [25]. These quantum chains are self-dual. At the self-dual point $\lambda = 1$ and for $N \to \infty$ they show an extended conformal symmetry with central charge $c = 2(n-1)/(n+2)$. Exact solutions of these $\mathcal{WA}_{n-1}$ Hamiltonian chains [26–29] have been obtained through Bethe ansatz techniques [28, 30]. Very recently, Cardy [31] has shown that a particular integrable perturbation of the critical $\mathcal{WA}_{n-1}$ models leads to self-dual chiral Potts models.

Since later we shall principally study the $\mathbb{Z}_3$ and $\mathbb{Z}_4$ versions of (1), we now list how $H^{(n)}$ specializes for these cases. If we keep insisting on Hermiticity, $H^{(3)}$ depends on three parameters apart from a normalization [13]. In accordance with (6) we write

$$H^{(3)} = -\frac{2}{\sqrt{3}} \sum_{j=1}^{N} \{ e^{-i\varphi/3} \sigma_j + e^{+i\varphi/3} \sigma_j^+ + \lambda (e^{-i\phi/3} \Gamma_j \Gamma_{j+1}^+ + e^{+i\phi/3} \Gamma_j^+ \Gamma_{j+1}) \}. \quad (8)$$

Here σ_j and Γ_j are 3×3 matrices acting at site j:

$$\sigma_j = \begin{pmatrix} 1 & 0 & 0 \\ 0 & \omega & 0 \\ 0 & 0 & \omega^2 \end{pmatrix}_j \qquad \Gamma_j = \begin{pmatrix} 0 & 0 & 1 \\ 1 & 0 & 0 \\ 0 & 1 & 0 \end{pmatrix}_j \quad (9)$$

and $\omega = \exp(2\pi i/3)$. We shall consider $0 \leqslant \lambda \leqslant \infty$; $0 \leqslant \phi, \varphi \leqslant \pi$ (for reflection properties of $H^{(3)}$ see [13]). In order not to get lost in three-dimensional diagrams, we shall often concentrate on two cases in which there is one relation between the three parameters: the integrable (INT) case, where the three parameters are related by equation (7), and the self-dual (SD) case where $\phi = \varphi$. For generic φ and λ, the self-dual case is not known to be integrable. The SD case contains the non-chiral limit $\varphi = \phi = 0$, in which we obtain the $\mathcal{WA}_2$ model, which coincides with the $\mathbb{Z}_3$-standard Potts model. It has a second-order phase transition at $\lambda = 1$, which for $N \to \infty$ is described by a conformal field theory with central charge $c = 4/5$ [32–34].

The phase diagram of the SD chiral $\mathbb{Z}_3$ model shows four different phases [22, 35, 36], see figure 1: for small chiral angle φ we have oscillating massive high- and low-temperature phases at $\lambda < 1$ and $\lambda > 1$, respectively, except for a small incommensurate phase interval around $\lambda = 1$. The two incommensurate phases appear centred around $\lambda = 1$ and become wider in λ as φ increases.

The Hermitian $\mathbb{Z}_4$-symmetric $H^{(4)}$ contains five parameters (again apart from a normalization), which we denote by λ, ϕ, φ, β and $\tilde{\beta}$:

$$H^{(4)} = -\sqrt{2} \sum_{j=1}^{N} \{ e^{-i\varphi/2} \sigma_j + \beta \sigma_j^2 + e^{i\varphi/2} \sigma_j^3 + \lambda [e^{-i\phi/2} \Gamma_j \Gamma_{j+1}^3 + \tilde{\beta} \Gamma_j^2 \Gamma_{j+1}^2 + e^{i\phi/2} \Gamma_j^3 \Gamma_{j+1}] \} \quad (10)$$

where σ_j and Γ_j are now 4×4 matrices obeying (3). For simplicity, and in agreement with (6), we shall consider only the case $\beta = \tilde{\beta} = 1/\sqrt{2}$, so that we have again two parameters for the non-self-dual integrable version, and two parameters λ and $\phi = \varphi$ for the self-dual case. For $\varphi = \phi = 0$ and $\beta = \tilde{\beta} = 1/\sqrt{2}$ the Hamiltonian (10) coincides with that of the Ashkin–Teller quantum chain [37] for the special value $h = 1/3$ in the notations of [38]. From the phase diagram of the Ashkin–Teller quantum chain we know that in the case $h = 1/3$ there is just one critical point at the self-dual value $\lambda = 1$. This is described by the $\mathcal{WA}_3$ rational model at $c = 1$, which has an extended conformal symmetry with fields of spin three and four.

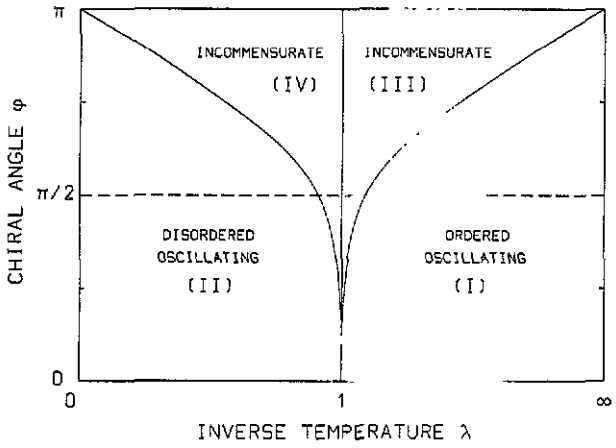

Figure 1. Schematic phase diagram of the self-dual $\mathbb{Z}_3$-chiral Potts model as defined in equation (8).

3. General results for the energy gaps of the $\mathbb{Z}_n$-chiral Potts model

Apart from the exact results for the non-chiral limiting case just mentioned at the end of the last section, there are many exact results for the superintegrable case (1), (4) (equivalent to (6) with $\varphi = \phi = \pi/2$): The $\mathbb{Z}_2$ case, which is the standard Ising quantum chain in a transverse field, has been solved in [10, 11, 39]. Recently, as mentioned above, the complete spectrum of the $\mathbb{Z}_3$-superintegrable quantum chain has also been calculated analytically [24]. We shall first collect some important partial results which are available for *generic* $\mathbb{Z}_n$.

In order to state these, we shall define all gaps with respect to the lowest $Q = 0, p = 0$ level, which we denote by $E_0(Q = 0, p = 0)$. Note that $E_0(Q = 0, p = 0)$ is not necessarily the ground state of the Hamiltonian. Depending on the parameters chosen, the ground state may be in any charge sector and may even have non-zero momentum p, since the model contains incommensurate phases. Nevertheless, in this section let us consider only gaps between $p = 0$ levels.

By $\Delta E_{Q,i}$ we denote the energy difference

$$\Delta E_{Q,i} = E_i(Q, p = 0) - E_0(Q = 0, p = 0) \tag{11}$$

where $E_i(Q, p = 0)$ is the ith level ($i = 0, 1, \ldots$) of the charge Q, momentum $p = 0$ sector. In the $\mathbb{Z}_2$(Ising) case of (1) it is well known that the lowest gap $\Delta E_{1,0}$ has the remarkable property of being linear in λ:

$$\Delta E_{1,0} = 2(1 - \lambda). \tag{12}$$

In 1983 Howes *et al* [13] found that the same is also true for the self-dual version of the $\mathbb{Z}_3$-chiral Potts model, equation (8) at the special chiral angle $\varphi = \phi = \pi/2$. They discovered this by calculating the high-temperature expansion up to tenth order in λ, finding that for these special angles all higher coefficients in the expansion, starting with the coefficient of λ^2, are zero.

In [14] it was the desire to generalize (12) so as to obtain for *all* $\mathbb{Z}_n$ and *all* Q the simple formula

$$\Delta E_{Q,0} = 2Q(1-\lambda) \qquad (\lambda < 1, Q = 1, \ldots, n-1) \tag{13}$$

which lead to the values (4) being chosen for the coefficients α_k and $\bar{\alpha}_k$ and to find the superintegrability of the model. In [14] the linearity of the gaps was checked through numerical calculations. The validity of (12) for the superintegrable $\mathbb{Z}_3$ model to all orders of a perturbation expansion in λ was first shown in [23] using a recurrence formula. Later, using analytic methods, Albertini *et al* [22, 23] for the superintegrable $\mathbb{Z}_3$ case, and then Baxter [20] for all superintegrable $\mathbb{Z}_n$, have calculated the lowest gaps of the Hamiltonian equation (1) in the thermodynamic limit $N \to \infty$.

Using the definition (11), Baxter's analytic results for the superintegrable model can be summarized in the form:

$$\Delta E_{Q=1,0} = 2(1-\lambda) \qquad (\lambda < 1) \tag{14}$$

$$\Delta E_{Q=0,1} = 2n(\lambda - 1) \qquad (\lambda > 1). \tag{15}$$

We now attempt to interpret the spectrum of (1) and the gap formula (13) in terms of particle excitations. Consider first equation (13). This would be obtained if the model contained only one single-particle species with mass $m_1 = 2(1-\lambda)$ and $\mathbb{Z}_n$ charge $Q = 1$. The lowest $\Delta Q \neq 1$ gaps would then arise from the thresholds of the scattering of Q of these $Q = 1$ particles.

In order to check whether it is correct to describe the spectrum at $\varphi = \phi = \pi/2$ this way, or whether more fundamental particles must be present, we shall study the zero momentum part of the spectrum as a function of the chiral angles, when these move away from the special superintegrable values. We shall start considering the spectrum down at $\varphi = \phi = 0$, where we know the particle structure from the thermally perturbed $\mathcal{WA}_{n-1}$ models and then move towards higher chiral angles.

The scaling regime around $\lambda = 1$ of the $\mathcal{WA}_{n-1}$ models is known to contain $n-1$ particle species, one in each of the non-zero $\mathbb{Z}_n$ charge sectors $Q = 1, \ldots, n-1$. The ratios of their masses m_Q are [40]:

$$\frac{m_Q}{m_1} = \frac{\sin(\pi Q/n)}{\sin(\pi/n)} \qquad (Q = 1, \ldots, n-1). \tag{16}$$

The particles with masses m_Q and m_{n-Q} form particle–antiparticle pairs. Near $\lambda = 1$ the mass scale m_1 behaves as

$$m_1 \sim (1-\lambda)^{(n+2)/2n} \tag{17}$$

as it follows from the conformal dimension $x = 4/(n+2)$ of the leading thermal operator of the $\mathcal{WA}_{n-1}$ model. Looking at (16), we can see that in the scaling $\mathcal{WA}_{n-1}$ model all particles are *isolated* non-degenerate levels in the spectrum of their respective charge sector. For example for the particle with mass m_Q to be on the scattering threshold of Q of the lightest particles with mass m_1, we must have $Q\sin(\pi/n) = \sin(Q\pi/n)$, which is possible only in the limit $n \to \infty$. Similarly, e.g. for $n \geqslant 5$, the m_4 particle is below the threshold $m_2 + m_2$, and approaches this threshold only as $n \to \infty$.

We now want to follow these single-particle levels in λ to outside the scaling region and as functions of the chiral angles φ and ϕ, in order to get information about what will happen at $\varphi, \phi \to \pi/2$. Since near $\lambda = 1$ the gaps can only be calculated numerically for generic ϕ, φ (we shall report such numerical calculations later), it is simplest to consider first the small-λ expansion for the lowest $p = 0$ gaps of the Hamiltonian (1). Using the coefficients in the form (6), but not assuming (7), to first order in λ we get

$$\Delta E_{Q,0} = \left(\sum_{k=1}^{n-1} \tilde{\alpha}_k (1 - \omega^{Qk})\right) - \lambda(\alpha_Q + \alpha_{n-Q}) + \cdots$$

$$= \left(\sum_{k=1}^{n-1} \frac{2\sin(\pi kQ/n)}{\sin(\pi k/n)} \sin\left(\left(\frac{2k}{n} - 1\right)\varphi + \frac{\pi kQ}{n}\right)\right)$$

$$- \frac{2\lambda}{\sin(\pi Q/n)} \cos\left(\left(\frac{2Q}{n} - 1\right)\phi\right) + \cdots. \tag{18}$$

Equation (18) fulfils the CP relation

$$\Delta E_{Q,i}(\lambda, \varphi, \phi) = \Delta E_{n-Q,i}(\lambda, -\varphi, -\phi) \qquad (i = 0, 1, \ldots). \tag{19}$$

In the sum in (18), the pairs of terms for k and $n - k$ are equal.

For $\varphi = 0$ and for $\varphi = \pi/2$ it is easy to simplify equation (18) using the trigonometrical sum formulae [41, 42]

$$\sum_{k=1}^{n-1} \sin\left(\frac{k\pi}{n}\right) = \cot\frac{\pi}{2n} \qquad \sum_{k=1}^{n-1} \sin^2\left(\frac{k\pi Q}{n}\right) = \frac{n}{2}$$

$$\sum_{k=1}^{n-1} \sin^3\left(\frac{k\pi}{n}\right) = \frac{1}{4}\left(3\cot\frac{\pi}{2n} - \cot\frac{3\pi}{2n}\right) \qquad \text{etc.} \tag{20}$$

For $\varphi = \phi = 0$ we obtain

$$\Delta E_{1,0} = 2\cot\frac{\pi}{2n} - \frac{2\lambda}{\sin(\pi/n)} + \cdots \tag{21}$$

and

$$\Delta E_{2,0} = 2\cot\frac{\pi}{2n} + 2\cot\frac{3\pi}{2n} - \frac{2\lambda}{\sin(2\pi/n)} + \cdots. \tag{22}$$

We identify

$$m_Q \equiv \Delta E_{Q,0} \tag{23}$$

and conclude from (16) and (22) that the mass ratio m_2/m_1 must decrease when going from the scaling region $\lambda \approx 1$ to $\lambda = 0$. For example for $n = 4$, equation (16) gives $m_2/m_1 = \sqrt{2}$, whereas at $\lambda = 1$ from (21) and (22) we get $m_2/m_1 \approx 1.17157$. Observe, that also according to (22), m_2 stays below the $Q = 2$ sector threshold at

$2m_1$ and, generally, the lowest levels of each charge sector remain isolated down to $\lambda = 0$.

We now examine how the perturbation formula (18) behaves in the superintegrable limit. Inserting $\varphi = \phi = \pi/2$, we obtain

$$\Delta E_{Q,0} = 2\sum_{k=1}^{n-1} \sin^2(\pi kQ/n) - \sum_{k=1}^{n-1} \sin(2\pi kQ/n)\cot(\pi k/n) - 2\lambda + \cdots. \tag{24}$$

The sums can be calculated explicitly, leading to the simple result

$$\Delta E_{Q,0} = 2(Q - \lambda) + O(\lambda^2). \tag{25}$$

Comparing (25) to (13), we have an apparent contradiction, since in (25) the factor Q is *not* multiplying λ.

Our detailed non-perturbative numerical analysis of the spectrum for the $\mathbb{Z}_3$ and $\mathbb{Z}_4$ cases (to be discussed in the next section) shows that the single-particle levels vary smoothly when increasing φ and ϕ starting from $\varphi = \phi = 0$. As soon as the chiral angles become non-zero, the particle–antiparticle pairs m_Q and m_{n-Q} split: m_1 decreases and m_{n-1} increases as φ and ϕ increase. Approaching $\varphi = \phi = \pi/2$, m_2 becomes twice as large as m_1, so that at $\varphi = \phi = \pi/2$, m_2 sits just at the $m_1 + m_1$ scattering threshold. So, our non-degenerate perturbation theory should break down for the channel $Q = 2$ at $\varphi, \phi \geqslant \pi/2$ [13], and, indeed we see this in the calculation of the λ^2 contribution to $\Delta E_{2,0}$. Because for general $\mathbb{Z}_n$ the explicit expression for the λ^2 term in (18) is too involved, here we specialize and give the result for the self-dual $\mathbb{Z}_3$ case. We find

$$\Delta E_{1,0}(\varphi, \lambda) = 4\sin\frac{\pi - \varphi}{3} - \frac{4\lambda}{\sqrt{3}}\cos\frac{\varphi}{3} + \lambda^2 f(\varphi) + O(\lambda^3) \tag{26}$$

where

$$f(\varphi) = -\frac{1}{3\cos\varphi}\left(2\sin\frac{\pi - 4\varphi}{3} - 4\sin\frac{\pi + 2\varphi}{3} + 3\sqrt{3}\right). \tag{27}$$

$f(\varphi)$ is smooth at $\varphi = \pi/2$ (we have $f(\pi/2) = -\sqrt{3}/2$), but it is singular for $\varphi \to -\pi/2$. Applying (19), from (26) we get $\Delta E_{2,0}$:

$$\Delta E_{2,0}(\varphi, \lambda) = 4\sin\frac{\pi + \varphi}{3} - \frac{4\lambda}{\sqrt{3}}\cos\frac{\varphi}{3} + \lambda^2 f(-\varphi) + O(\lambda^3). \tag{28}$$

While formula (26) for $\Delta E_{1,0}$ can be used in the whole range $0 \leqslant \varphi < \pi$ (considering non-negative φ), the corresponding expression (28) is valid only for $0 \leqslant \varphi < \pi/2$ and diverges at $\varphi = \phi = \pi/2$. The λ^2 contribution to the analogous $\mathbb{Z}_4$ formula will be given in section 5. It shows a similar divergence in the expression for m_2.

Since (28) breaks down at $\varphi = \pi/2$, we need further information in order to decide whether the $Q = 2$ particle survives at and beyond $\varphi = \pi/2$. This then will clarify the question as to whether the single-particle picture described above makes sense at the superintegrable line.

4. Finite-size numerical calculation of the low-lying spectrum of the $\mathbb{Z}_3$-chiral quantum chain

4.1. Convergence exponent y

We shall now describe several detailed numerical checks of the two-particle picture from the spectrum in the high-temperature massive region of the $\mathbb{Z}_3$ model. For this purpose, we have calculated numerically the eight lowest $p = 0$ levels of each charge sector of the Hamiltonian (8) for $N = 2, \ldots, 12$ sites. While in the last section, we concentrated on the single-particle levels, now we shall also examine the scattering states and check whether the corresponding thresholds appear as expected.

For chains of up to $N = 8$ sites we are able to diagonalize $H^{(3)}$ exactly. Using Lanczos diagonalization we can use up to $N = 12$ sites. We shall always give the results for periodic boundary conditions, but we have also partially checked the results with twisted boundary conditions. The extrapolation to $N \to \infty$ is done using both the Van-den-Broeck–Schwartz algorithm [43] and rational approximants [44] (for details on the application to quantum chains and error estimation see [45]).

Neighbouring higher levels sometimes cross over as functions of the number of sites N, so that for these there is a danger of connecting wrong sequences. This can be controlled by calculating the leading power of the convergence, y, defined by

$$\Delta E(N) - \Delta E(\infty) = N^{-y} + \cdots \tag{29}$$

and checking the smoothness of the approximants y_N:

$$y_N = -\ln\left(\frac{\Delta E(N) - \Delta E(\infty)}{\Delta E(N-1) - \Delta E(\infty)}\right) \Big/ \ln\left(\frac{N}{N-1}\right). \tag{30}$$

In (29) and (30), $\Delta E(N)$ is a gap $\Delta E_{Q,i}$ calculated for N sites.

The calculation of y_N is also very useful for distinguishing between single-particle levels and two or more particle scattering states. For single-particle levels we expect

$$\Delta E(N) - \Delta E(\infty) = \exp(-N/\xi) + \cdots \tag{31}$$

i.e. exponential convergence in N (ξ is a correlation length), so that for these the y_N should increase very fast with N. In contrast to this, for two-particle states we should have a power behaviour in N, more precisely, we should have $\lim_{N\to\infty} y_N = 2$.

4.2. The spectrum for the superintegrable case $\varphi = \pi/2$

We first discuss our numerical results for the $\mathbb{Z}_3$-superintegrable case $\phi = \varphi = \pi/2$. Table 1 lists results for 16 low-lying gaps for $\lambda = 0.5$ in the high-temperature regime, where from (12) we know that $m_1 \equiv \Delta E_{Q=1,0} = 1$. As we have checked by repeating the calculation for several other values of $\lambda < 1$, this value $\lambda = 0.5$ is not special regarding the structure of the spectrum. However, there is the nice feature that because of (13) for this λ the gaps should approach integer values in the limit $N \to \infty$.

In the $Q = 1$ sector we see an isolated lowest state at $m_1 = 2(1 - \lambda)$ followed by a bunch of levels at $4m_1$. Looking at table 2 which gives the convergence with N as parametrized by y according to (29), we see that, indeed, the m_1 level ($Q = 1$;

Table 1. The lowest energy gaps $\Delta E_{Q,i}$, as defined in equation (11), for the $\mathbb{Z}_3$-Hamiltonian equation (8) and the superintegrable case $\varphi = \phi = \pi/2$, $\lambda = 0.50$. The numbers given in brackets indicate the estimated error in the last written digit. All calculations of the gaps have been performed to 12-digit accuracy and using all $N = 2, \ldots, 12$ sites for the extrapolation $N \to \infty$. In order to save space, in the tables we give less digits and omit the low-N data. Details on our determination of the exponent of convergence y, defined in (29), (30) are given in table 2. In the last line of each table, we give our particle interpretation of the various levels, as deduced from the result for y.

N	$i=1$	2	3	4	5	6	7
$\Delta E_{Q=0,i}$							
7	3.159 898 3	4.835 958 5	4.452 038 1	5.930 367 6	5.903 224 0	7.048 703 0	6.355 779 7
8	3.111 564 9	4.424 092 3	4.207 536 7	5.486 866 4	5.549 671 4	6.398 752 1	6.033 870 1
9	3.080 841 7	4.121 328 0	4.016 833 4	5.125 288 0	5.238 409 1	5.857 252 4	5.724 369 7
10	3.060 413 7	3.895 466 2	3.866 160 5	4.829 732 6	4.970 082 5	5.412 117 4	5.442 370 1
11	3.046 316 6	3.724 480 9	3.745 565 2	4.586 779 5	4.740 600 4	5.047 110 4	5.191 719 5
12	3.036 280 6	3.593 205 8	3.647 837 9	4.385 696 0	4.544 674 0	4.747 164 5	4.971 466 9
∞	2.9998(3)	2.986(7)	3.01(1)	3.02(8)	3.05(6)	2.9(1)	2.95(8)
y	3.0(1)	2.9(2)	2.0(1)	2.1(1)	1.9(1)	2.8(6)	?
	$3m_1$	$3m_1$	m_1+m_2	m_1+m_2	m_1+m_2	$3m_1$	?

N	$i=0$	1	2	3	4
$\Delta E_{Q=1,i}$					
7	0.998 487 4	4.517 308 5	5.790 549 1	6.604 971 1	6.161 256 6
8	0.999 428 9	4.376 002 3	5.477 543 2	6.078 524 2	5.845 634 7
9	0.999 804 4	4.280 997 2	5.234 916 1	5.675 775 3	5.587 014 8
10	0.999 940 5	4.215 075 0	5.044 256 2	5.365 276 5	5.374 967 2
11	0.999 985 1	4.168 055 6	4.892 453 2	5.123 574 3	5.200 236 8
12	0.999 997 8	4.133 696 2	4.770 087 2	4.933 509 3	5.055 264 4
∞	1.000 000 0	3.99(2)	4.00(1)	4.01(5)	4.01(3)
y	expon.	3.0(2)	2.0(1)	2.9(2)	1.9(1)
	m_1	$2m_1+m_2$	$2m_2$	$2m_1+m_2$	$2m_2$

N	$i=0$	1	2	3	4	5
$\Delta E_{Q=2,i}$						
7	1.999 572 6	2.790 137 3	4.379 824 5	5.663 341 7		6.129 486 9
8	1.999 676 1	2.638 990 5	4.025 634 4	5.310 688 5	6.042 583 4	5.846 839 0
9	1.999 830 4	2.526 108 9	3.735 181 8	4.969 775 3	5.832 310 3	5.648 737 9
10	1.999 924 7	2.439 960 7	3.497 015 2	4.658 310 8	5.576 691 9	5.506 540 0
11	1.999 970 1	2.372 939 1	3.300 895 8	4.380 869 4	5.311 057 7	5.402 260 4
12	1.999 989 3	2.319 894 8	3.138 407 1	4.136 597 7	5.052 792 3	5.324 297 0
∞	2.0001(1)	2.002(7)	2.00(5)	2.0(1)	2.6(5)	4.99(1)
y	expon.	2.0(1)	1.9(1)	1.9(2)	?	2.9(2)
	m_2	$2m_1$	$2m_1$	$2m_1$	?	m_1+2m_2

column $i = 0$) shows exponential convergence, whereas the levels $Q = 1$; $i = 1, 2$ converge as N^{-3} and N^{-2}, respectively. This indicates that the $i = 1$ level is due to three-particle $(m_1 + m_1 + m_1)$ scattering, and the $i = 2$ level due to two-particle $(m_2 + m_2)$ scattering, as shown in the bottom line in table 1.

The $Q = 2$ sector shows no isolated ground state, but starts with a bunch of levels around $\Delta E = 2$. There is strong evidence for another bunch around $\Delta E = 5$, of which table 1 shows just the first level. The convergence for the further $\Delta E = 5$ levels is poor and we do not give the numbers. A clue to the nature of the $\Delta E = 2$

Table 2. Exponents y_N of the convergence $N \to \infty$ as defined in equation (30), for the $\mathbb{Z}_3$-superintegrable case and $\lambda = 0.5$ for the lower levels given in table 1. 'expon.' means that the fast increasing sequence of the y_N indicates exponential convergence.

	y_N for $\Delta E_{Q=0,i}$				y_N for $\Delta E_{Q=1,i}$			y_N for $\Delta E_{Q=2,i}$		
N	$i=1$	2	3	4	$i=0$	1	2	$i=0$	1	2
7	2.6413	1.7475	1.2814	1.0998	5.6670	2.1812	1.3354		1.5124	1.0720
8	2.6955	1.9024	1.3808	1.2290	7.2946	2.3893	1.4389	2.0775	1.5900	1.2068
9	2.7348	2.0293	1.4594	1.3340	9.0948	2.4728	1.5230	5.4923	1.6503	1.3140
10	2.7646	2.1348	1.5222	1.4212	11.2974	2.5376	1.5917	7.7025	1.6973	1.4013
11	2.7879	2.2232	1.5731	1.4947	14.5079	2.5883	1.6482	9.6994	1.7340	1.4733
12	2.8067	2.2976	1.6148	1.5573	21.8070	2.6287	1.6948	11.7909	1.7633	1.5334
∞	3.0(1)	2.9(2)	2.0(1)	2.1(1)	expon.	3.0(2)	2.0(1)	expon.	2.0(1)	1.9(1)

levels is found through their convergence for increasing N. Table 2 shows clearly that the level labelled $Q = 2; i = 0$ has an N-dependence which drastically differs from that of the other levels, indicating that this is the level of a single particle with mass $m_2 = 4(1 - \lambda)$ (we have checked the λ-dependence repeating the calculation for six other values of λ). So, we can answer the question posed at the end of the last section: the m_2 level can be clearly seen in the superintegrable case, although it lies at the edge of the scattering threshold. The power-behaved $Q = 2$ states at $\Delta E = 2$ should then be interpreted as $m_1 + m_1$ states. The level $Q = 2$; $i = 5$ may be $m_1 + m_2 + m_2$, which has the correct total $\mathbb{Z}_3$-charge $Q = 2$.

The pattern at $Q = 0$, $\Delta E = 3$ is as expected by this picture. There should be $m_1 + m_2$ states and $m_1 + m_1 + m_1$ states, both distinguished by different values of y, as observed in tables 1 and 2.

For other values of λ ranging from $\lambda = 0.2$ to $\lambda = 0.8$ we find precisely the same structure. Not surprisingly, above $\lambda = 0.8$ the convergence with respect to N becomes poor, since the relevant mass scale m_1 vanishes as $\lambda \to 1$ and so at $\lambda = 0.8$ it is already quite small.

4.3. The spectrum off the superintegrable line

After having found a simple two-particle pattern in the superintegrable case, we now check how this structure is modified for $\varphi, \phi \neq \pi/2$. In order not to vary too many parameters, we consider only the INT and SD cases defined at the end of section 2. For the INT case explicit formulae for the spectrum are not yet available (for some first attempts, see [46]). For the SD case there may be no integrability at all. So, for the following, there is currently no alternative to our numerical or perturbative methods.

We start with the SD case. In section 3 we discussed the perturbation expansion of the lowest gaps to order λ^2. This indicated that increasing φ from the Potts value $\varphi = 0$ to $\varphi = \pi/2$ for fixed $\lambda < 1$ decreases the mass m_1 and increases m_2 until for $\varphi = \pi/2$ we reach the value $m_2/m_1 = 2$. Above $\varphi = \pi/2$ we should then have $m_2/m_1 > 2$ which makes it difficult to isolate the $Q = 2$ particle in the $m_1 + m_1$ continuum (if it is there at all). Figure 2 shows the different patterns which we expect in the three charge sectors for $\varphi < \pi/2$ (left-hand side) and for $\varphi > \pi/2$ (right-hand side). The extrapolation of the finite-size numbers reported in table 3 confirms all details of these expected patterns. For $\varphi = 2\pi/3$, among the three lowest $Q = 2$ levels at $\Delta E = 2m_1$ we see no exponentially converging level. For $\varphi > \pi/2$ all

thresholds are determined by m_1 alone, these are $3m_1$, $4m_1$ and $2m_1$ for $Q = 0$, 1, 2 sectors, respectively.

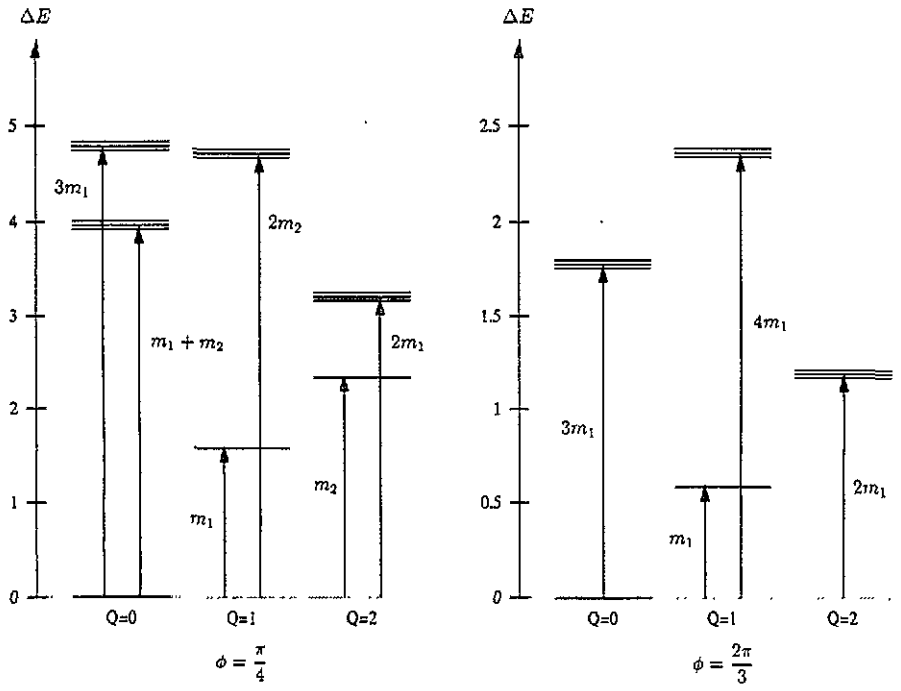

Figure 2. Level structure for the self-dual $\mathbb{Z}_3$-chiral Potts model in the high-temperature massive region: left-hand side, for a chiral angle $\varphi < \pi/2$ (below the superintegrable value); right-hand side, $\varphi > \pi/2$ (above the superintegrable value). In the latter case the thresholds are determined by m_1 alone.

Table 3. The lowest energy gaps $\Delta E_{Q,i}$ (extrapolated $N \to \infty$) of the self-dual $\mathbb{Z}_3$-model (8), for $\lambda = 0.5$ and two values of φ: $\varphi = \pi/4$ (below the superintegrable line), and $\varphi = 3\pi/2$ (above the superintegrable line), together with their particle interpretation.

$\phi = \varphi = \pi/4$, $\lambda = 0.5$				$\phi = \varphi = 2\pi/3$, $\lambda = 0.5$			
Q	i	$\Delta E_{Q,i}(\infty)$	Particles	Q	i	$\Delta E_{Q,i}(\infty)$	Particles
0	1	3.9150(2)	$m_1 + m_2$	0	1	1.75(1)	$3m_1$
0	2	3.85(3)	$m_1 + m_2$	0	2	1.80(5)	$3m_1$
0	3	3.98(4)	$m_1 + m_2$	0	3	1.8(1)	$3m_1$
0	4	4.70(8)	$3m_1$	1	0	0.5868(2)	$\equiv m_1$
0	5	3.90(5)	$m_1 + m_2$	1	1	2.36(4)	$4m_1$
1	0	1.583 436 6(1)	$\equiv m_1$	2	0	1.174(2)	$2m_1$
1	1	4.68(1)	$2m_2$	2	1	1.18(2)	$2m_1$
2	0	2.339 607(1)	$\equiv m_2$	2	2	1.19(5)	$2m_1$
2	1	3.168(4)	$2m_1$				
2	2	3.17(5)	$2m_1$				

In order to see whether the $Q = 2$ particle survives in the $\varphi > \pi/2$ region, we have to look for more and higher levels. For *small* λ we know from equation (28) (supposing this to be still valid) where to search for m_2 at $\varphi > \pi/2$, and so we have looked slightly above the superintegrable line at $\varphi = 7\pi/12$, $\lambda \leqslant 0.25$ among the eight lowest levels for a rapidly converging one. Indeed, as is shown in table 4, the level $i = 6$ of the table converges much faster than its neighbours. So, it is a good candidate for the m_2 level. However, with increasing λ this convergence diminishes quite fast and an even/odd N hopping takes over. This may be due to the increasing instability of the m_2 particle.

Table 4. Selected $Q = 2$ gaps for $\varphi = 7\pi/12$ (slightly above the superintegrable line) of the self-dual $\mathbb{Z}_3$-model. The numbering of the levels ($i = 0, \ldots$) refers to $N = 12$ sites, for a smaller number of sites there are fewer levels between $i = 0$ and $i = 5$. The values of m_1 are very well determined because of fast convergence. Observe that the $i = 0$-levels converge excellently to $2m_1$. In both cases level $i = 6$ converges much faster with N than the other levels, which may indicate that this is the m_2 level. Non-monotonic behaviour in N is common in the neighbourhood of the incommensurate phase.

	$\Delta E_{Q=2,i}(\varphi = 7\pi/12, \lambda = 0.10)$ $m_1 = 1.503\,358\,45$				$\Delta E_{Q=2,i}(\varphi = 7\pi/12, \lambda = 0.15)$ $m_1 = 1.411\,316\,11$			
N	$i = 0$	5	6	7	$i = 0$	5	6	7
7	3.039 19	3.586 23	3.892 05	7.994 16	2.867 77	3.636 50	3.950 76	7.699 24
8	3.032 22	3.726 96	3.893 48	7.904 58	2.858 47	3.855 81	3.980 85	7.578 93
9	3.027 27	3.656 40	3.892 85	7.837 88	2.851 77	3.752 62	3.961 89	7.490 35
10	3.023 63	3.743 32	3.893 13	7.786 99	2.846 78	3.895 47	3.979 10	7.423 10
11	3.020 88	3.693 94	3.893 01	7.747 32	2.842 97	3.818 57	3.967 35	7.370 73
12	3.018 75	3.751 71	3.893 06	7.715 79	2.839 99	3.918 01	3.977 95	7.329 05

For $\varphi < \pi/2$ the threshold in the $Q = 0$ sector also depends on m_2, being $m_1 + m_2$. The left column of table 3 shows that the numerical values for the various thresholds come out very well and that, for example, $m_2/m_1 = 1.477\,55$ at $\varphi = \pi/4$ and $\lambda = 0.5$. Unfortunately, the determination of the corresponding values for y is quite unsafe, since for $\varphi \neq \pi/2$ we have no exact values for $\lim_{N\to\infty} \Delta E_i$ available as we had in the superintegrable case from (13). So the results we obtain for the y_N depend strongly on the very unprecise extrapolated results which are used for $\Delta E_i(\infty)$.

4.4. The integrable case for $\varphi \neq \pi/2$

Turning now to the integrable case INT, our data in table 5 show the same pattern as in the SD case, only the convergence is less good (for the sake of brevity we have omitted the finite-size data). It is not clear whether the $\Delta E_{Q=2,0}$ level converges exponentially at all. This result is somewhat surprising, because one might have expected behaviour which was more clearly particle-like in the integrable case. We recall that nothing is known about the integrability of the general SD case.

There is not much difference between the SD case (table 3) and the INT case (table 5). For example observe that in the right-hand part of table 5, which gives an example for chiral angles above the superintegrable value, the low-lying gaps come out clearly as integer multiples of the single scale m_1, as is expected for threshold values

Table 5. Lowest energy gaps $\Delta E_{Q,i}$ as in table 3, but for two different choices of the parameters in the *integrable* $\mathbb{Z}_3$-model case, in which φ and ϕ are related by (7). On the left-hand side we give an example with chiral angles below the superintegrable case, on the right-hand side ϕ,φ are taken above their superintegrable values. The pattern observed here is very similar to that of the self-dual case in table 3.

$\varphi = \pi/4$, $\phi = 19.47\ldots$(deg) $\lambda = 0.75$				$\varphi = 2\pi/3$, $\phi = 135.58\ldots$(deg) $\lambda = 0.70$			
Q	i	$\Delta E_{Q,i}(\infty)$	Particles	Q	i	$\Delta E_{Q,i}(\infty)$	Particles
0	1	1.933(2)	$m_1 + m_2$	0	1	1.50(1)	$3m_1$
0	2	1.9(2)	$m_1 + m_2$	0	2	1.53(5)	$3m_1$
0	3	1.8(3)	$m_1 + m_2$	1	0	0.495(2)	$\equiv m_1$
1	0	0.750(1)	$\equiv m_1$	1	1	1.99(1)	$4m_1$
1	1	2.41(2)	$2m_2$	2	0	0.995(1)	$2m_1$
2	0	1.19(2)	$\equiv m_2$	2	1	1.00(1)	$2m_1$
2	1	1.50(3)	$2m_1$	2	2	1.04(5)	$2m_1$
				2	3	2.52(5)	$5m_1$

if $m_2 > 2m_1$. The numerical precision is not very good because in the neighbourhood of the incommensurate phase the finite-size approximants to, for example, m_1 first fall with N and then rise again, a property which is not easy to handle by usual extrapolation procedures.

Apart from the just mentioned non-monotonous behaviour of the gaps for increasing N, the onset of the incommensurate phase is not felt in our study of the $p = 0$ levels even at $\varphi = \phi = 5\pi/6$, $\lambda = 0.5$. For still larger angles, it becomes difficult and then practically impossible to arrange the gaps for various N into plausible sequences. Anyway, it is already surprising that for $\varphi = \pi/2$ and higher, the low $p = 0$ gaps do not seem to take any notice of the incommensurate phase boundary, and vanish smoothly for $\lambda \to 1$.

In the low-temperature regime $\lambda > 1$ the pattern of the lowest levels is the same in all three charge sectors. As expected, in the limit $N \to \infty$ the ground state is threefold degenerate (one isolated level in each charge sector). Above the ground state we find for $\varphi < \pi/2$ a gap which is $\lambda(m_1(\lambda^{-1}) + m_2(\lambda^{-1}))$. Then we see a quite dense sequence of levels starting after a gap of $3\lambda m_1(\lambda^{-1})$ (the same gap in all three charge sectors). If we would have normalized $H^{(3)}$ including a factor $\sqrt{\lambda}$ in the denominator of (8), the gaps would be just the same as those in the $Q = 0$ sector at the duality reflected value of λ. This is a generalization of Baxter's result (15) for the superintegrable case to $\varphi < \pi/2$.

5. Perturbative and finite-size numerical results for the spectrum of the chiral $\mathbb{Z}_4$-quantum chain

In the last section we reported our numerical evidence for a two-particle picture of the spectrum of the off-critical chiral $\mathbb{Z}_3$-Potts quantum chain. In this section we shall give analogous numerical evidence for a three-particle structure in the high-temperature regime of the chiral $\mathbb{Z}_4$-Potts quantum chain.

We start giving the high-temperature expansion of the lowest gaps of the self-dual $\mathbb{Z}_4$-quantum chain up to order λ^2. It reads explicitly

$$\Delta E_{1,0} = 2(1 + 2\sin\tfrac{1}{4}(\pi - 2\varphi)) - 2\lambda\sqrt{2}\cos(\varphi/2) + \lambda^2 g(\varphi) + \cdots \tag{32}$$

$$\Delta E_{2,0} = 4\sqrt{2}\cos(\varphi/2) - 2\lambda + \lambda^2 h(\varphi) + \cdots \tag{33}$$

$$\Delta E_{3,0} = 2(1 + 2\sin\tfrac{1}{4}(\pi + 2\varphi)) - 2\lambda\sqrt{2}\cos(\varphi/2) + \lambda^2 g(-\varphi) + \cdots \tag{34}$$

where g and h are the following functions

$$g(\varphi) = \frac{1 + \sqrt{2}\sin(\varphi/2)}{2\sin((2\varphi + \pi)/4)} + \frac{4\sin^2\varphi + 5\sin\varphi - 8\sqrt{2}\cos(\varphi/2) - 1}{4\sqrt{2}\cos\varphi\cos(\varphi/2)} \tag{35}$$

$$h(\varphi) = -\frac{2}{\cos\varphi}(1 - \sqrt{2}\cos(\varphi/2) + 2\cos^2(\varphi/2)). \tag{36}$$

The function $h(\varphi)$ is singular for $\varphi \to \pi/2$, similarly, $g(\varphi)$ is singular for $\varphi \to -\pi/2$. Of course, (34) follows from (32) by a CP transformation, see (19). At $\varphi = \phi = 0$ the sectors $Q = 1$ and $Q = 3$ are degenerate.

At $\varphi = 5\pi/6$ and $\lambda = 0$, according to (32) the gap $\Delta E_{1,0}$ vanishes, and above this value of φ the ground state of the system is in the $Q = 1$ sector. This feature is due to the particular choice $\beta = 1/\sqrt{2}$ which we made after (10). If we consider more general β, then this ground-state level crossing moves to $\varphi = \pi/2 + 2\sin^{-1}(\beta/\sqrt{2})$. So, for $\beta \geqslant 1$ the ground state remains in the sector $Q = 0$ up to $\varphi = \pi$.

For φ above its superintegrable value $\varphi = \pi/2$ (with $\beta = 1/\sqrt{2}$) the scattering thresholds in all sectors are determined by $m_1 \equiv \Delta E_{1,0}$ alone, and the 'single-particle gaps' equations (33) and (34) move above the scattering thresholds in the sectors $Q = 2$ and $Q = 3$, respectively. This is quite analogous to what happened in the $Q = 2$ sector of the $\mathbb{Z}_3$ model.

For all $\lambda > 0$ the $Q = 2$ gap is larger than both the $Q = 1$ and $Q = 3$ gaps. For small values of λ both $\Delta E_{1,0}$ and $\Delta E_{2,0}$ decrease with increasing φ, while $\Delta E_{3,0}$ grows. At $\varphi = \pi/2$ the gaps are integer-spaced.

The high-temperature expansion is reliable for small λ and the lowest levels only. So, for larger values of λ, we have numerically calculated the six lowest $p = 0$ levels of each charge sector for the Hamiltonian (10). In the $\mathbb{Z}_4$ case we are able to handle up to $N = 10$ sites only. Correspondingly, the extrapolations are less precise than in the case of $\mathbb{Z}_3$.

First, we present our results for some low-lying levels in the spectrum for the superintegrable case of (10): $\varphi = \phi = \pi/2, \beta = \bar{\beta} = 1/\sqrt{2}$. Table 6 contains the results at $\lambda = 0.5$, where from (13) we should have $m_1 = 1$, so that we expect the gaps for $N \to \infty$ to approach simple integers. Indeed, this comes out well from our numbers. As before, we have checked for four other values of λ to ensure that there is nothing special about choosing $\lambda = 0.5$.

In each of the $Q \neq 0$ sectors we see one level which shows very fast convergence with N, and we identify this with the single-particle state of mass $m_Q = Q$.

In the charge sector $Q = 0$ we can evaluate the four lowest gaps precisely enough to assign them to $\Delta E = 4$. There should be four different types of scattering states: $m_1 + m_1 + m_1 + m_1$, $m_1 + m_1 + m_2$, $m_2 + m_2$ and $m_1 + m_3$. While the exponents determine the first two types, we would have to move away from $\varphi = \phi = \pi/2$ in order to distinguish the two latter states. In the sector $Q = 1$ we see two excited states in addition to the m_1-particle state. They could be one three-particle and one two-particle scattering state, both with $\Delta E = 5$. This is compatible with the expected states $m_1 + m_2 + m_2$ and $m_2 + m_3$.

Table 6. The lowest energy gaps $\Delta E_{Q,i}$, as in table 1, but here instead of the $\mathbb{Z}_3$ case now for the $\mathbb{Z}_4$-Hamiltonian equation (10). Superintegrable case $\phi = \varphi = \pi/2$ for $\lambda = 0.5$. Note the overshooting in the approximants for m_1 and m_2.

	$\Delta E_{Q=0,i}$				$\Delta E_{Q=1,i}$		
N	$i=1$	2	3	4	$i=0$	1	2
4	4.487 034 9	6.640 119 8	6.938 600 0	7.120 252 7	0.978 226 0	6.290 750 1	8.818 234 3
5	4.244 383 5	6.207 984 4	6.344 834 7	6.439 078 6	0.993 217 3	5.733 938 6	7.935 567 2
6	4.135 299 6	5.690 777 0	5.928 017 2	6.020 875 9	0.998 579 4	5.442 921 2	7.224 546 3
7	4.080 781 7	5.319 141 5	5.546 939 6	5.727 887 5	0.999 956 4	5.280 982 6	6.809 831 1
8	4.051 162 5	5.047 703 3	5.260 617 8	5.288 090 5	1.000 144 0	5.186 013 2	6.455 040 9
9	4.033 965 7	4.846 046 4	4.958 244 7	5.042 728 8	1.000 092 7	5.127 743 2	6.187 583 6
10	4.023 430 6	4.693 653 4	4.724 880 3	4.874 467 2	1.000 039 0	5.090 539 8	5.983 404 5
∞	4.0000(2)	3.89(2)	3.9(9)	3.7(4)	1.0001(1)	4.97(3)	5.7(6)
y	4.0(2)	2.1(3)	2.9(4)	1.6(1)	expon.	3.5(3)	1.8(1)
	$4m_1$	$2m_2$ or m_1+m_3	$2m_1+m_2$	$2m_2$ or m_1+m_3	m_1	?	m_2+m_3

	$\Delta E_{Q=2,i}$		$\Delta E_{Q=3,i}$		
N	$i=0$	1	$i=0$	1	2
4	1.976 098 1	3.634 488 1	3.009 030 9	5.070 687 3	5.413 524 3
5	1.988 558 3	3.195 114 1	2.997 859 2	4.489 924 4	4.929 744 3
6	1.995 997 2	2.902 770 8	2.998 022 4	4.104 839 3	4.552 086 2
7	1.998 935 1	2.701 308 8	2.999 127 7	3.841 238 7	4.263 614 2
8	1.999 827 8	2.558 280 4	2.999 720 9	3.655 860 2	4.043 246 3
9	2.000 021 3	2.453 947 6	2.999 937 9	3.522 247 5	3.873 346 2
10	2.000 033 0	2.375 911 1	2.999 996 4	3.423 704 6	3.740 633 6
∞	2.000 01(3)	1.9(1)	3.000 01(6)	2.8(2)	3.02(4)
y	expon.	1.9(1)	expon.	2.1(2)	1.7(2)
	m_2	$2m_1$	m_3	m_1+m_2	m_1+m_2

The numerical convergence of the scattering levels and the possibility of ordering the levels into clear sequences in N gets worse if we consider the sectors $Q = 2$ and $Q = 3$. In the bottom line of table 6 we give a few quite safe assignments.

We now look numerically at how this particle pattern is modified if we choose values of the parameters $\phi \neq \pi/2$, $\varphi \neq \pi/2$ for which no analytic results are available. In table 7 we have collected the first few lowest energy gaps for three choices of the parameters.

First, we look at values of $\phi = \varphi < \pi/2$. For $\phi = \varphi = \pi/4$ (which is half-way to the $\mathcal{W}$-point) and $\lambda = 0.5$ the masses of the m_2 and m_3 states are clearly below the scattering thresholds and the remaining levels can be excellently explained as multi-particle states. In the charge-sector $Q = 2$ there is one state with $\Delta E = 4.6$ which seems to be unexplained by this pattern. However, the extrapolation $N \to \infty$ is quite delicate and therefore the errors may be too small. Thus, this state could also be a $2m_1$ state.

If we choose $\phi = \varphi > \pi/2$, the low-lying levels of the spectrum are given by m_1 alone. However, for small values of λ and ϕ slightly above the superintegrable line the $Q = 2$ charge sector shows a high level that converges very rapidly and is not an integral multiple of m_1. The middle part of table 7 contains the explicit values for $\phi = \varphi = 3\pi/5$ and $\lambda = 0.10$. Here, the m_2 particle is still clearly visible as a high level in the $Q = 2$ sector. Unfortunately, the m_3 particle is not visible in the

Table 7. The left and middle parts of this table show a selection of lowest energy gaps of the self-dual, but not super-integrable $\mathbb{Z}_4$-Hamiltonian for two different choices of the parameters $\phi = \varphi$, with $\beta = \bar{\beta} = 1/\sqrt{2}$ and different λ. The right-hand part of the table contains an example of the INT case. For most levels in this table the determination of the convergence exponent y is very unsafe due to the considerable uncertainty in $\Delta E_{Q,i}(\infty)$. So, as in tables 3 and 5, the particle content is inferred almost exclusively from $\Delta E_{Q,i}(\infty)$ alone.

$\phi = \varphi = \pi/4$ $\lambda = 0.50$				$\phi = \varphi = 3\pi/5$ $\lambda = 0.10$				$\varphi = \pi/4$, $\phi = 19.47\ldots$(deg) $\lambda = 0.75$			
Q	i	$\Delta E_{Q,i}(\infty)$	Particles	Q	i	$\Delta E_{Q,i}(\infty)$	Particles	Q	i	$\Delta E_{Q,i}(\infty)$	Particles
0	1	5.77(2)	$m_1 + m_3$	0	1	5.1(2)	$4m_1$	0	1	2.767(4)	$m_1 + m_3$
0	2	5.76(8)	$m_1 + m_3$	1	0	1.2116781	$\equiv m_1$	0	2	3.2(1)	$2m_1 + m_2$
0	3	7.1(2)	$2m_2$	1	1	6.1(3)	$5m_1$	1	0	0.8663(1)	$\equiv m_1$
1	0	2.033 83(1)	$\equiv m_1$	2	0	2.42334(7)	$2m_1$	1	1	3.50(1)	$2m_1 + m_3$
1	1	7.1958(4)	$m_2 + m_3$	2	1	2.430(6)	$2m_1$	2	0	1.529(2)	$\equiv m_2$
1	2	6.98(7)	$m_2 + m_3$	2	5	3.211450(1)	$\equiv m_2$	2	1	1.8(1)	$2m_1$
2	0	3.4282(1)	$\equiv m_2$	3	0	3.6349(5)	$3m_1$	3	0	1.786(2)	$\equiv m_3$
2	1	4.15(6)	$2m_1$					3	1	2.52(7)	$3m_1$
2	2	4.59(1)	?								
2	3	7.62(7)	$2m_3$								
3	0	3.7501(1)	$\equiv m_3$								
3	1	5.458(2)	$m_1 + m_2$								

$3m_1$ continuum.

The right column of table 7 shows that basically the same patterns can also be observed in the INT case although here the approximation is less good.

To summarize, our numerical data support a three-particle interpretation of the low-lying spectrum for the chiral $\mathbb{Z}_4$-Potts quantum chain with φ in the range from 0 to slightly above $\pi/2$.

6. Energy–momentum relations for the single-particle states

When interpreting the excitations of the model in terms of particles, we should also look for their energy–momentum dispersion rule. On a lattice with N sites and periodic boundary conditions, the momentum p can take the N values

$$p = -[\tfrac{1}{2}N], \ldots, -1, 0, 1, \ldots, [\tfrac{1}{2}N]. \tag{37}$$

In calculating the limit $N \to \infty$ we use

$$P = \frac{2\pi}{N} p \qquad (-\pi \leqslant P \leqslant \pi). \tag{38}$$

Apart from the $\mathcal{WA}_{n-1}$ case $\phi = \varphi = 0$ the Hamiltonian (1) does not conserve parity, so, in general, the curves $E(P)$ will not be symmetrical with respect to $P \to -P$.

An expansion to first order in λ gives a first orientation of the energy–momentum relation near $\lambda = 0$ for generic $\mathbb{Z}_n$. In an easy generalization of (18) we find, for $Q \neq 0$,

$$\begin{aligned} \Delta E_{Q,0} &= \left(\sum_{k=1}^{n-1} \tilde{\alpha}_k (1 - \omega^{Qk}) \right) - \lambda (\mathrm{e}^{\mathrm{i}P} \alpha_Q + \mathrm{e}^{-\mathrm{i}P} \alpha_{n-Q}) + \cdots \\ &= \left(\sum_{k=1}^{n-1} \tilde{\alpha}_k (1 - \omega^{Qk}) \right) - \frac{2\lambda}{\sin(\pi Q/n)} \cos(P - P_{\mathrm{m}}) + \cdots \end{aligned} \tag{39}$$

where

$$P_{\mathrm{m}} = (1 - 2Q/n)\phi. \tag{40}$$

In the second line of (39) we have inserted the definition (6) of α_k in the λ-dependent term. Since, to first order in λ, the first term of (39) contains no P-dependence, we see that, in the high-temperature limit, the violation of parity in the dispersion relation of the particle with charge Q is exclusively due to the presence of a macroscopic momentum P_{m} as given in (40). A particle and its antiparticle feel macroscopic momenta which are opposite in sign.

In the parity-conserving case $\varphi = \phi = 0$ the system can be made isotropic between space and Euclidian time rescaling the Hamiltonian by a suitable λ-dependent factor ξ. So, for $\varphi = \phi = 0$ the particle will have the energy–momentum relation of the lattice Klein–Gordon equation

$$E/\xi = \sqrt{\mu_Q^2 + K^2} \tag{41}$$

or

$$E^2 = m_Q^2 + \xi^2 K^2 \tag{42}$$

where ξ is the rescaling factor, and we write

$$K = 2\sin(P/2) \qquad m_Q = \mu_Q \xi. \tag{43}$$

The correct conformal normalization factor ξ for the $\mathcal{WA}_{n-1}$ quantum chains at the critical point $\lambda = 1$ is well known [27, 34]:

$$\xi(\lambda = 1) = n. \tag{44}$$

Using formulae (39) and (21), (22), the m_Q and the rescaling factors for the $Q = 1$ and $Q = 2$ particles of the $\mathcal{WA}_{n-1}$ chains near $\lambda = 0$ can be calculated explicitly. The m_Q for $Q = 1, 2$ have been given in (21), (22) and (23), from which we find

$$\Delta E_{1,0} = 2\cot\left(\frac{\pi}{2n}\right) - \frac{2\lambda}{\sin(\pi/n)}\left(1 - \frac{K^2}{2}\right) + \cdots \tag{45}$$

$$\Delta E_{2,0} = 2\cot\left(\frac{\pi}{2n}\right) + 2\cot\left(\frac{3\pi}{2n}\right) - \frac{2\lambda}{\sin(2\pi/n)}(1 - K^2/2) + \cdots \tag{46}$$

from which we get different rescaling factors for particles with different charge. Defining

$$\zeta = n\sqrt{\lambda} \tag{47}$$

(coinciding for $\lambda = 1$ with (44)), for small λ we obtain

$$\xi_{Q=1}(\lambda) = \frac{\sqrt{2}}{n\sin(\pi/2n)}\zeta + \cdots \tag{48}$$

and

$$\xi_{Q=2}(\lambda) = \frac{\xi_{Q=1}(\lambda)}{\sqrt{2\cos^2(\pi/2n) - \frac{1}{2}}} + \cdots. \tag{49}$$

Putting in numbers, we find that the main variation of the ξ_Q over the whole range $0 \leqslant \lambda < 1$ is determined (for low values of n) up to 10...20% by the factor ζ. For example for $\mathbb{Z}_4$ at $\lambda \to 0$ we have

$$\lim_{\lambda\to 0} \xi_{Q=1}/\zeta = 0.923\,88\ldots \qquad \lim_{\lambda\to 0} \xi_{Q=2}/\zeta = 0.840\,90\ldots \tag{50}$$

similarly for higher n. For the Ising case $n = 2$ we have exactly $\xi_{Q=1} = \zeta$ for all λ [47].

For $\varphi = \phi = 0$ the two parameters ξ and m_Q determine the dispersion curve exactly. For example in the $\mathcal{WA}_2$ case ($n = 3$) we find for $\lambda = 0.00$, 0.25, 0.50, 0.75, 0.90:

$$\frac{m_Q}{(1-\lambda)^{5/6}} = 3.464\,101\,62 \qquad 3.585\,828\,24(1) \qquad 3.674\,214(2)$$

$$3.73(3) \qquad 3.8(1) \tag{51}$$

and

$$\frac{\xi}{\zeta} = 0.942\,809\,0 \qquad 0.975\,170\,2(1) \qquad 0.996\,697(2) \qquad 1.008(6) \qquad 1.00(1) \tag{52}$$

respectively. At $\lambda = 0.75$ and $\lambda = 0.9$ we observe non-monotonic behaviour for the levels with N which gives rise to a considerable uncertainty in the extrapolation $N \to \infty$. At lower values of λ the exponential convergence has already clearly set in below $N = 12$ sites, so that there we may trust the extrapolation.

For $\lambda \to 0$ the masses determining the N convergence go to infinity. So for $\lambda = 0$ there is no N-dependence, once a minimal value of N, dictated by the nearest-neighbour interaction, is reached. This is in agreement with (48) and (49) and shows that the high-temperature expansion around $\lambda = 0$ at the same time is also a non-relativistic expansion of (41). For the $\mathcal{WA}_2$ case we have checked that the order λ^2 term of (45) agrees with the second-order expansion term of (41). We find

$$\Delta E_{1,0} = \frac{2}{\sqrt{3}}(3 - \lambda(2 - K^2) - \lambda^2(1 - K^2 + K^4/6) + \cdots) \tag{53}$$

which fits to the form

$$\Delta E_{1,0} = m_1 + (\xi K)^2/(2m_1) - (\xi K)^4/(8m_1^3) + \cdots. \tag{54}$$

So, certainly to this order, the momentum dependence of the $\mathcal{WA}_2$ single-particle level m_1 is that of the Klein–Gordon equation (41) or (42).

We have no physical interpretation as to why, for low n, the ratio ξ_Q/ζ varies so little with λ (in the $n = 2$ case we have $\xi \equiv \zeta$), and we find it strange for the particle interpretation that, in general, $\xi_Q(\lambda)$ is Q-dependent.

For the $\mathbb{Z}_3$-superintegrable case Albertini *et al* [22] have given analytic formulae and plots of the energy–momentum dependence of the m_1 particle in the high-temperature range $0 \leqslant \lambda < 1$, and for the first $Q = 0$ excitation in the low-temperature range $\lambda > 1$. Here we want to give simple approximate expressions for the dispersion curves of both $Q = 1$ and $Q = 2$ particles, not only for the superintegrable, but also for the general self-dual $\mathbb{Z}_3$-chiral model at $0 \leqslant \lambda \leqslant 1$.

For $\varphi, \phi > 0$ we have no simple analytic form for the dispersion equation and so we have performed fits to the curves $E(P)$ given by

$$E(P) = \sum_{m=0}^{3} a_m \cos^m(P - P_m) + \sum_{m=1,3} b_m \sin^m(P - P_m) \tag{55}$$

which are good up to $\lambda \approx 0.6$. Table 8 collects some of these fitted coefficients.

For $\lambda < 0.5$ the convergence in N is excellent for all p if we use up to $N = 12$ sites. For $\lambda \leqslant 0.1$ we can nicely fit the data for the momentum dispersion of the $Q = 1$ particle just using equation (39). For larger values of λ inspection of the numerical curves and the fits in table 8 shows that P_m decreases with increasing λ and, in addition, the curves start becoming unsymmetrical with respect to $P = P_m$. The larger the angle φ, and the larger λ is the more terms in the expansion (55) are needed for a reasonable fit. Figures 3 to 5 show momentum distributions for various values of λ and φ together with our fitted curves. As is seen from figure 5, for $\varphi = 2\pi/3$ and $\lambda = 0.5$ more terms in the expansion would have been needed. As we approach the incommensurate region, e.g. at $\varphi = 5\pi/6$, $\lambda = 0.3$, other levels are below the m_1 level at $|P| > \pi/2$, so that the identification of the m_1 dispersion curve becomes difficult. It may be that in this region new particle types will show up.

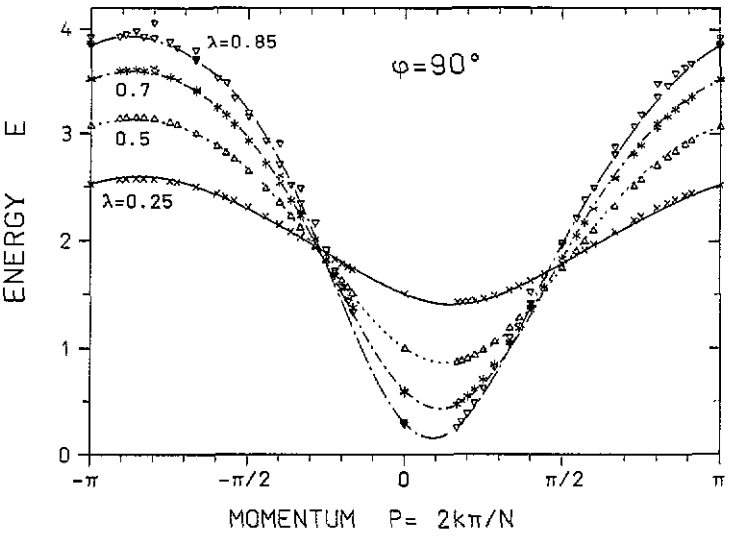

Figure 3. Energy–momentum relation of particle m_1 for the $\mathbb{Z}_3$-superintegrable case and various values of the inverse temperature λ in the high-temperature region. The small crosses and triangles are finite-size values calculated for $N = 6, \ldots, 12$ sites.

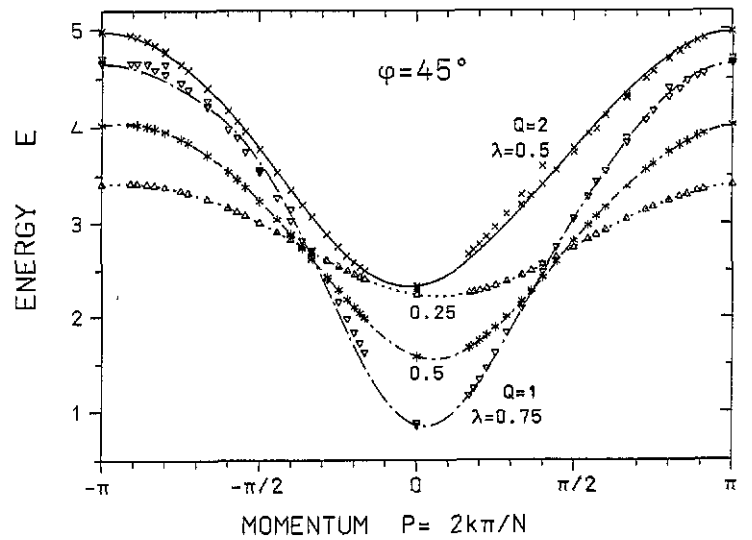

Figure 4. Same as figure 3, but for φ below the superintegrable value and both for m_1 (three broken curves) and m_2 (full curve).

7. Conclusions

We have shown that the low-lying spectrum of the massive high-temperature regime of the self-dual $\mathbb{Z}_n$-Potts quantum chain at low chiral parameter values $\varphi \lesssim 2\pi/3$ can be described in terms of $n-1$ particles which carry $\mathbb{Z}_n$ charges $Q = 1, \ldots, n-1$

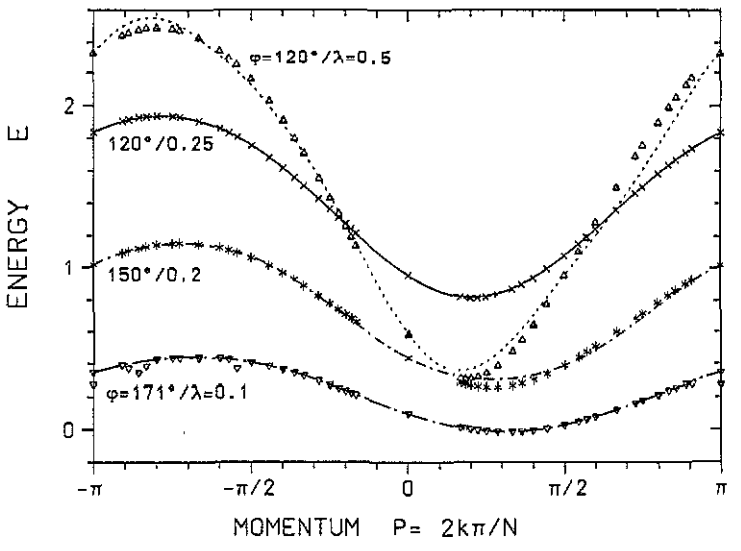

Figure 5. Same as figure 3, but for several values of φ above the superintegrable value (towards the incommensurate region), for the $Q = 1$ particle m_1. The shift of the minima of the curves to the right due to the macroscopic momentum P_m is clearly seen.

Table 8. Coefficients of fits to the energy–momentum relation equation (55) for various φ and λ, all for the self-dual model. Except for the last line, which is for the lowest $Q = 2$ gap, all other fits are for the lowest $Q = 1$ gaps. The quality of the fits can be judged from figures 3, 4 and 5. In the last column we quote φ_m, which we define by $P_m = \varphi_m/3$.

φ (deg)	λ	a_0	a_1	a_2	a_3	b_1	b_3	φ_m (deg)
45	0.25	2.8745	−0.5924	−0.0549	−0.0075	0.0033		39
45	0.50	3.0302	−1.1653	−0.2355	−0.0764	−0.0134		30
45	0.75	3.3502	−1.6702	−0.6028	−0.2300	0.0864	−0.2121	18
90	0.25	2.0436	−0.5118	−0.0412	−0.0848	−0.0112		81
90	0.50	2.2363	−1.1331	−0.2381	0.0014	−0.0188		69
90	0.70	2.4363	−1.4587	−0.4244	−0.1190	−0.0757	−0.0112	57
90	0.85	2.6161	−1.5982	−0.5752	−0.2791	−0.1981	−0.0745	39
120	0.25	1.4317	−0.5570	−0.0552	−0.0022	−0.0263		105
120	0.50	1.5407	−0.8112	−0.0909	−0.2517	−0.3291		57
150	0.20	0.7281	−0.4696	−0.0028	0.0451	0.0013		150
171	0.10	0.2257	−0.2260	−0.0128	−0.0009			171
45	0.50	3.7927	−1.1973	−0.1501	−0.0874	−0.3223		−45

(we denote their masses by m_Q). This is seen by studying the variation of the single-particle masses from their Köberle–Swieca values at zero chirality $\varphi = 0$ up to and above the superintegrable value $\varphi = \pi/2$. For low-inverse temperatures λ we use a perturbation expansion. For higher λ we concentrate on the special cases $n = 3$ and $n = 4$ and diagonalize the Hamiltonian numerically.

In the $\mathbb{Z}_3$ case the mass ratio m_2/m_1 is shown to rise continuously from $m_2/m_1 = 1$ at $\varphi = 0$ to $m_2/m_1 = 2$ for the superintegrable case $\varphi = \pi/2$. In the superintegrable case the $Q = 2$ particle appears precisely at the $m_1 + m_1$ scattering

threshold. For $\varphi \to \pi$, m_1 tends to zero. How far the $Q = 2$ particle survives for $\varphi > \pi/2$ is not clear. In table 5 we give evidence that the $Q = 2$ single-particle level is still present up to $\lambda = 0.15$ and $\varphi = 7\pi/12$. In the superintegrable case we identify two- and three-particle scattering states through their different power behaviour in the chain size N. The two single-particle levels show exponential convergence in N. The perturbation expansion of m_2 is shown to diverge at order λ^2 for $\varphi \to \pi/2$.

At small λ, the non-conservation of parity in the model results only in the appearance of a Q-dependent macroscopic momentum $P_m = (1 - 2Q/n)\phi$ in the energy–momentum dispersion relations of the particles, which is $P_m = \pm\phi/3$ in the $\mathbb{Z}_3$ case. Our numerical data suggest that the average P_m decreases with increasing λ, perhaps $P_m \to 0$ for $\lambda \to 1$, but we have no simple parametrization of the effects of parity violation at large λ and restrict ourselves to giving trigonometrical fit coefficients.

Using the same methods we have also verified in detail that the high-temperature massive spectrum of the chiral $\mathbb{Z}_4$-Potts quantum chain can be described analogously in terms of three massive particles with $\mathbb{Z}_4$-charges $Q = 1$, 2 and 3. In the superintegrable case the mass ratio equals the ratio of the charges, such that now both the $Q = 2$ and $Q = 3$ particles appear at scattering thresholds. As before, the scattering states can easily be identified by their power behaviour in the chain length N, while the single particles show exponential convergence with N.

It would be interesting to use Lüscher's [48] method to obtain numerical information on the phase-shifts or the S-matrix from the N-dependence of the multi-particle states.

References

[1] Ostlund S 1981 *Phys. Rev.* B **24** 398
[2] Huse D A 1981 *Phys. Rev.* B **24** 5180
[3] Einstein T L 1987 *Proc. 10th Johns Hopkins Workshop* ed K Dietz and V Rittenberg (Singapore: World Scientific) p 17
[4] den Nijs M 1988 *Phase Transitions and Critical Phenomena* vol 12, ed C Domb and J L Lebowitz (New York: Academic) p 219
[5] Selke W 1988 *Phys. Rep.* **170** 213
[6] von Gehlen G and Rittenberg V 1984 *Nucl. Phys.* B **230** 455
[7] Everts H U and Röder H 1989 *J. Phys. A: Math. Gen.* **22** 2475
[8] Marcu M, Regev A and Rittenberg V 1981 *J. Math. Phys.* **22** 2740
[9] Centen P, Rittenberg V and Marcu M 1982 *Nucl. Phys.* B **205** 585
[10] Fradkin E and Susskind L 1978 *Phys. Rev.* D **17** 2637
[11] Kogut J B 1979 *Rev. Mod. Phys.* **51** 659
[12] Vescan T, Rittenberg V and von Gehlen G 1957 *J. Phys. A: Math. Gen.* **19** 1957
[13] Howes S, Kadanoff L P and Den Nijs M 1983 *Nucl. Phys.* B **215** 169
[14] von Gehlen G and Rittenberg V 1985 *Nucl. Phys.* B **257**[FS14] 351
[15] Dolan L and Grady M 1982 *Phys. Rev.* D **25** 1587
[16] McCoy B M 1991 *Special Functions ICM 90, Satellite Conf. Proc.* ed M Kashiwara and T Miwa (Berlin: Springer) p 245
[17] Onsager L 1944 *Phys. Rev.* **65** 117
[18] Davies B 1990 *J. Phys. A: Math. Gen.* **23** 2245
[19] Roan Sh-Sh 1991 Onsager's algebra, loop algebra and chiral Potts model *Preprint* MPI für Mathematik Bonn, September 1991
[20] Baxter R J 1988 *Phys. Lett.* **133A** 185; 1989 *J. Stat. Phys.* **57** 1; 1990 *Phys. Lett.* **146A** 110; 1988 *J. Stat. Phys.* **52** 639
[21] Zamolodchikov A B 1989 *Int. J. Mod. Phys.* A **4** 4235

[22] Albertini G, McCoy B M and Perk J H H 1989 *Phys. Lett.* **135A** 159; 1989 *Phys. Lett.* **139A** 204; 1989 *Adv. Stud. Pure Math.* **19** 1
[23] Au-Yang H, McCoy B M, Perk J H H, Tang Sh and Yan M L 1987 *Phys. Lett.* **123A** 219
[24] Dashmahapatra S, Kedem R and McCoy B M M 1993 Spectrum and completeness of the 3 state superintegrable chiral Potts model *Preprint* Stony Brook ITP-SB 92-11
[25] Fateev V A and Zamolodchikov A B 1985 *Sov. Phys.–JETP* **62** 215; 1985 (Engl. Trans. *Zh. Eksp. Teor. Fiz.* **89** 380)
[26] Alcaraz F C 1986 *J. Phys. A: Math. Gen.* **19** L1085; 1987 *J. Phys. A: Math. Gen.* **20** 2511
[27] Alcaraz F C 1990 *J. Phys. A: Math. Gen.* **23** L1105
[28] Alcaraz F C and Lima Santos A 1986 *Nucl. Phys.* B **275** 436
[29] Fateev V A and Lykyanov S 1988 *Int. J. Mod. Phys.* A **3** 507
[30] Tsvelick A M 1988 *Nucl. Phys.* B **305** 675
[31] Cardy J L 1992 Critical exponents of the chiral Potts model from conformal field theory *Preprint* Cambridge UCSBTH-92-37
[32] Dotsenko Vl S 1984 *Nucl. Phys.* B **235** 54
[33] Friedan D, Qiu Z and Shenker S 1984 *Phys. Rev. Lett.* **52** 1575
[34] von Gehlen G, Rittenberg V and Ruegg H 1985 *J. Phys. A: Math. Gen.* **19** 107
[35] von Gehlen G and Krallmann T 1993 *Preprint* Bonn to appear
[36] von Gehlen G 1993 Phase diagram and two-particle structure of the $\mathbb{Z}_3$-chiral Potts model *Preprint* Bonn HE-92-18
[37] Kohmoto M, den Nijs M and Kadanoff L P 1981 *Phys. Rev.* B **24** 5229
[38] Baake M, von Gehlen G and Rittenberg V 1987 *J. Phys. A: Math. Gen.* **20** L479
[39] Pfeuty P 1970 *Ann. Phys.* **57** 79
[40] Köberle R and Swieca J A 1979 *Phys. Lett.* **86B** 209
[41] Gradstein I S and Ryshik I M 1965 *Tables of Integrals, Series and Products* (New York) equations (1.344) and (1.351)
[42] Henkel M and Lacki J 1989 *Phys. Lett.* **138A** 105
[43] Van den Broek J M and Schwartz L W 1979 *SIAM J. Math. Anal.* **10** 658
[44] Burlirsch R and Stoer J 1964 *Numer. Math.* **6** 413
[45] Henkel M and Schütz G 1988 *J. Phys. A: Math. Gen.* **21** 2617
[46] McCoy B M and Roan Sh-Sh 1990 *Phys. Lett.* **150A** 347
[47] von Gehlen G 1991 *J. Phys. A: Math. Gen.* **24** 5371
[48] Lüscher M and Wolff U 1990 *Nucl. Phys.* B **339** 222
Lüscher M 1986 *Commun. Math. Phys.* **104** 177; 1986 *Commun. Math. Phys.* **105** 153